Op-Amp based analog implementation of the Integral Resonant Control scheme

E. Pereira[1], S. O. R. Moheimani[2]*, and S. S. Aphale[3]

[1] Department of Electrical, Electronic and Control Engineering, University of Castilla-La Mancha, Spain

[2]* School of Electrical Engineering and Computer Science, The University of Newcastle, Callaghan, NSW, Australia
(Corresponding Author: reza.moheimani@newcastle.edu.au)

[3] Centre for Applied Dynamics Research (CADR), School of Engineering, Kings College, University of Aberdeen, UK.

ABSTRACT

The Integral Resonant Control (IRC) is a simple low-order control scheme that has been introduced as a high-performance controller design methodology for flexible structures with collocated actuator-sensor pairs. It is capable of achieving significant damping, over several modes, while guaranteeing closed-loop stability of the system in presence of unmodelled out-of-bandwidth dynamics. These reasons make the IRC an ideal controller for various industrial damping applications, if packaged in a simple easy-to-implement electronic module. In this work, we propose an analog implementation of the IRC scheme using a single Op-Amp circuit. The goal is to demonstrate that with a simple analog realization of the modified IRC scheme, it is possible to damp a large number of vibration modes. A brief discussion about the modeling, circuit considerations, implementation and experimental results is presented in order to validate the usefulness and practicality of the proposed analog IRC implementation.

Keywords: Smart structures, vibration control, analog implementation, piezoelectric materials

1. INTRODUCTION

A variety of industrial, scientific and defense applications employ flexible structures [1, 2, 3, 4]. These structures are prone to unwanted vibrations. Thus, vibration control of flexible structures has been an active research field, see [5, 6, 7]. An interesting property of the smart structures with collocated sensor-actuator pairs is that the phase of their frequency response lies continuously between 0º and 180º. Various vibration damping techniques exploiting this property have been proposed by researchers in the past. Velocity feedback achieves damping by using this property to implement a very simple derivative controller [8]. In practive however, implementation of this controller results in relatively low performance and poor phase margins. Resonant control is another approach that has been applied successfully to collocated highly resonant systems [9, 10, 11]. As its response does not roll-off at higher frequencies, this control technique may not be suitable in certain applications. To alleviate this problem, positive position feedback (PPF) has been proposed and experimentally demonstrated [12, 13]. The main drawback of control techniques such as PPF and resonant control is that they produce a second-order controller to damp a single resonant mode of the structure, thus resulting in a high-order controller for damping multiple modes. Also, they may be difficult to tune for cases where more than one mode is to be controlled. An easyto-tune, low-order damping controller, that imparts adequate damping to multiple modes, without instability issues due to unmodeled system dynamics, was the main motivation for proposing the Integral Resonant Control

(IRC) approach in [14].

The IRC is a highly effective, yet a very straightforward control design methodology. The implementation reported in [14] utilizes a real-time DSP system to implement a controller with a simple structure. In this work, we demonstrate the analog implementation of the IRC scheme using a single operational amplifier circuit. It is shown that this analog circuit delivers the expected damping performance over multiple resonant modes and is robust to unmodeled high-frequency dynamics of the structure. The analog circuit implementation of the IRC scheme presented and tested in this paper, has the potential to be utilized in various industry based damping applications, owing to its good damping performance, simplicity of design, and ease of tuning and inexpensive nature.

1-1. Preliminaries

Collocated flexible structures have the pole-zero interlacing property. Therefore, the phase of their transfer function lies between 0º and 180º ([15, 16]). The IRC scheme takes advantage of this property in order to damp multiple vibration modes with a simple, low-order controller. Transfer function of a collocated system can be represented as the sum of many second-order blocks, i.e.

$$G(s) = \sum_{i=0}^{M} \frac{\alpha_i}{s^2 + 2\xi_i\omega_i + \omega_i^2} . \tag{1}$$

All manuscripts where $\alpha_i > 0$ and $\forall i$ and M→∞ [17]. For all practical purposes, a truncated model with a constant additive feed-through term is used. This approach captures the system dynamics within the bandwidth of interest with sufficient accuracy and accounts for the effect of high-frequency modes on low frequency zeros of the system [18]. This truncated model can be written as,

$$G(s) = \sum_{i=0}^{N} \frac{\alpha_i}{s^2 + 2\xi_i\omega_i + \omega_i^2} + D , \tag{2}$$

where D is the additive feed-through term and N is the number of in-bandwidth modes. The implementation of the IRC is presented in the next section. Experimental results are included Section in 3. Finally, in Section 4 the main conclusions are listed.

2. IMPLEMENTATION

A cantilever beam, similar to the one in reference [14], is used to test the analog implementation of IRC (see Fig 1). The control scheme proposed in [14] is shown in Fig 2(a). The feed-through term ($D_f < 0$), which is a negative real number, places a pair of low-frequency complex conjugate zeros between the origin and the first pair of complex conjugate poles of the system (G_{yu}). Thus, the system can be controlled with an integrator in positive feedback ($K < 0$), since the phase of (K/s)G_{yu} is kept between −90º and 90º. This approach deems the system sensitive to low frequency disturbances such as D.C. offsets. In this work, we present an equivalent control scheme that alleviates this problem; see Fig 2(b). The resulting equivalent controller can be written as:

$$C(s) = \frac{K}{s + KD_f} . \tag{3}$$

Note that as K and D_f are negative numbers and the equivalent control scheme is a lossy integrator with positive feedback. Then, the controller can be realized with the single operational amplifier circuit illustrated in Fig 3. That is, $C(s)$ can be parameterised as:

$$C(s) = \frac{1/(R_1 C)}{s + 1/(R_2 C)} \tag{4}$$
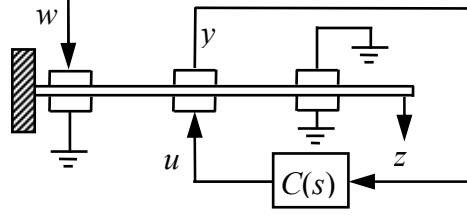
Figure 1. Experimental platform, where _u_ is the input and _y_ is the output of the collocated patch, _w_ is the disturbance patch and _z_ is the tip velocity

(a) **(b)**
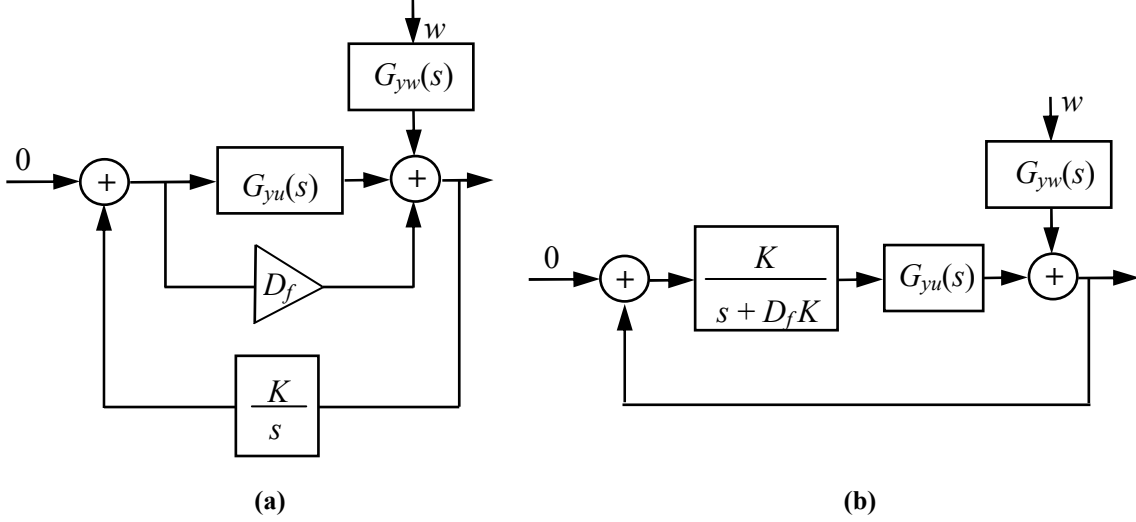
Figure 2. (a) Control scheme proposed in [14], where D_f is the feed-through term and K is the integral term. (b) Equivalent representation of the IRC scheme where D_f and K are grouped into a lossy integrator

where R_1, R_2 and C are the elements of the lossy integrator circuit [19]. As the DC loop gain is negative, the phase of $C(s)G_{yu}(s)$ starts from 180°. In addition, the phase of G_{yu} lies between 0° and 180° and the phase of $C(s)$ is between 0° and 90°. Then, the system of Fig 2(b) is stable if and only if the DC loop gain is less than 1 [20]. The controller parameters are tuned in a stepwise fashion described as follows (For a detailed discussion and analysis of this scheme, the reader is referred to [14]):

 • Choose the value of the capacitance C and the resistance R_2 to agree with the bandwidth constraints obtained from the root locus plot.
 • Tune the gain of the controller with the resistance R_1.
 • Cancel the output offset of the controller with the resistance R_3, where $R_3 = R_2 \| R_1$.

3. RESULTS

Transfer functions $G_{zw}(s)$, $G_{zu}(s)$, $G_{yw}(s)$ and $G_{yu}(s)$ were obtained using a Polytec scanning laser vibrometer (PSV-300). The idea is to design and wrap a controller around $G_{yu}(s)$ and impart damping to $G_{zw}(s)$. This is possible since both the transfer functions have identical poles. Using a subspace-based system identification technique, an accurate model of the experimental system was obtained [21]. This transfer function captures the system dynamics within the bandwidth of interest, with sufficient accuracy and can be written as:

$$C(s) = \frac{0.045s\left(s^2 + 0.8s + 2925\right)\left(s^2 + 4s + 1.1\cdot10^5\right)\left(s^2 + 11s + 8.3\cdot10^5\right)}{(s+5)\left(s^2 + 0.8s + 2799\right)\left(s^2 + 4s + 1.0\cdot10^5\right)\left(s^2 + 11s + 7.9\cdot10^5\right)} \qquad (5)$$
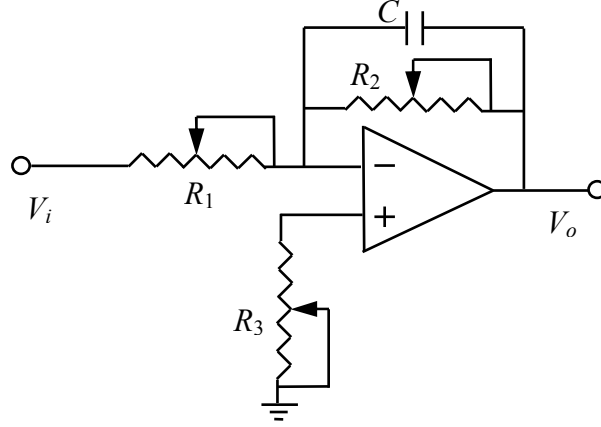
Figure 3. Analog circuit implementing the modified IRC scheme. V_i is the input and V_o is the output of the controller, C is the capacitance and R_1, R_2 and R_3 are the resistances used for tuning the controller
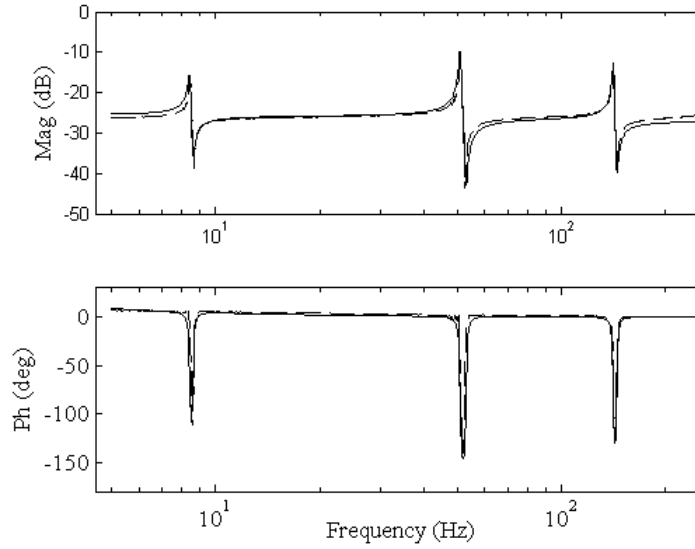
Figure 4. Magnitude (dB) and phase (deg) response of the measured (- -) and modelled system (—) of G_{yu}

The frequency response functions (FRF) of the measured and modelled system of $G_{yu}(s)$ are plotted in Fig 4. Note that Eq. 5 describes the dynamics of the collocated system (of the form given in Eq. 2) augmented with the dynamics of the sensor given by:

$$\frac{V_i}{V_p} = \frac{s}{s + \left(R_p + R_i\right)\big/\left(R_p R_i C\right)} \tag{6}$$

For an analog implementation, it is necessary to fully understand the various circuit parameters and their effects on the overall system. Fig 5 shows the equivalent electrical model of the analog controller and the pair of collocated piezoelectric transducers.

The K and D_f parameters for the equivalent controller $C(s)$ implemented in this work can be obtained using the methodology discussed in [14]. The sensor dynamics must be taken into account in order to implement the modified IRC scheme presented here. To explain the difference between the design of the modified control scheme with and without the sensor dynamics, the root locus plots for $C(s)G_{yu}(s)$ for both cases are shown in Fig 6. Neglecting the sensor dynamics, the controller bandwidth governed by p_C has no adverse effect on the closed-loop stability of the system; see Fig 6(a). However, when the sensor dynamics are taken into account, as in Fig 6(b), p_C can makes the system unstable. Then, the bandwidth of the controller is increased (by placing the pole p_C further away from the $j\omega$ axis). In this case, the damping performance increases up to some extent. Any increase in the controller bandwidth beyond this point results in system instability. On the other hand,

Flexible beam
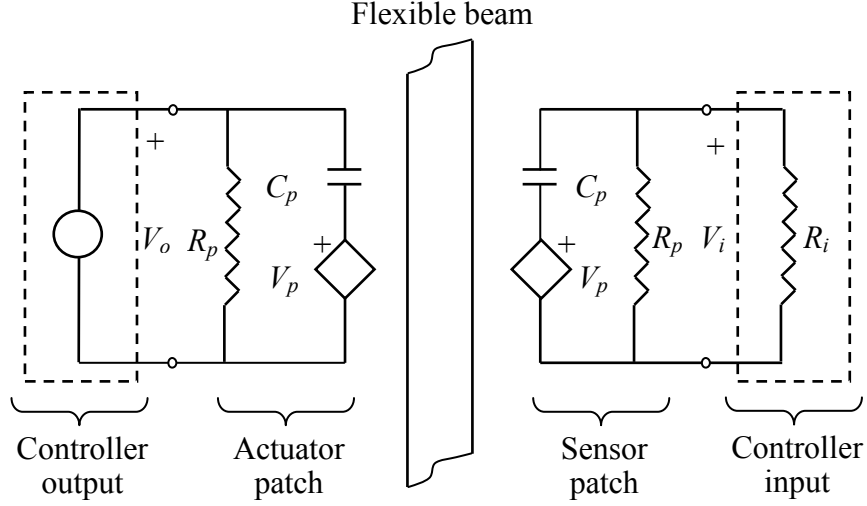
Figure 5. Electrical model of the analog controller and the pair of collocated piezoelectric transducers. Here, C_p and R_p are the capacitance and the resistance of the piezoelectric sensor. At the sensor side, the circuit can be modelled by a resistor R_i

(a)

(b)
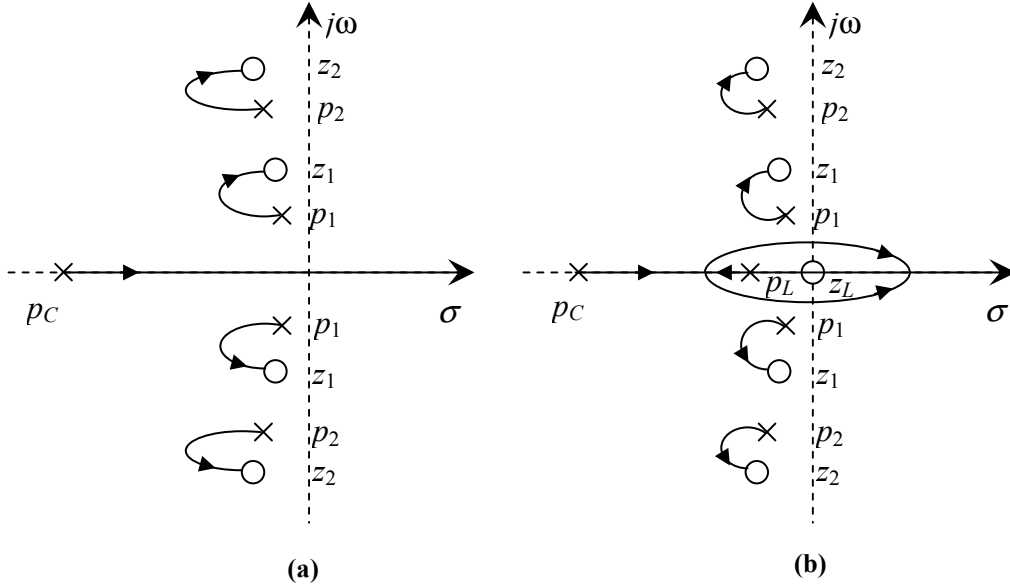
Figure 6. Root locus plots of the system without (a) and with (b) the sensor dynamics, where the poles and zeros of the model given by Eq. (2) are $(p_1, \cdots, p_i)$ and $(z_1, \cdots, z_i)$ respectively. The pole of the controller is (p_C) while (p_L) and (z_L) are the pole and zero of the sensor dynamics

reducing the bandwidth of the controller (by placing the pole p_C closer to the $j\omega$ axis) results in poor damping performance. Thus, there is a tradeoff between the maximum damping that can be imparted to the system and the controller bandwidth. The Bode plot of the system $C(s)G_{yu}(s)$ with $D_fK = 226.2$ and $1/D_f = -18$, is plotted in Fig 7. It can be seen that the phase of $C(s)G_{yu}(s)$ does not start from $180°$, and the gain margin depends on the bandwidth of the controller. Thus, as the bandwidth of the controller increases, the gain margin decreases and vice versa.

The controller was implemented with a general purpose operational amplifier, MC33078. Based on the tuning criterion explained earlier, a 3.3nF ceramic capacitor was chosen to obtain the necessary bandwidth constraint. The resistance R_2 was realized and tuned using a 2MΩ potentiometer while R_1 and R_3 were implemented using 100KΩ potentiometers. After tuning the controller, its measured 3dB cut-off bandwidth was found to be 36Hz and the D.C. gain was 18.

Fig 8 shows the experimental open-loop and closed-loop responses of G_{zw}. Fig 9(a) shows the FRF of G_{zw} in open and closed-loop for the first nine vibration modes. Although the controller is designed based on a model with only three vibration modes, it achieves attenuation at higher freque-
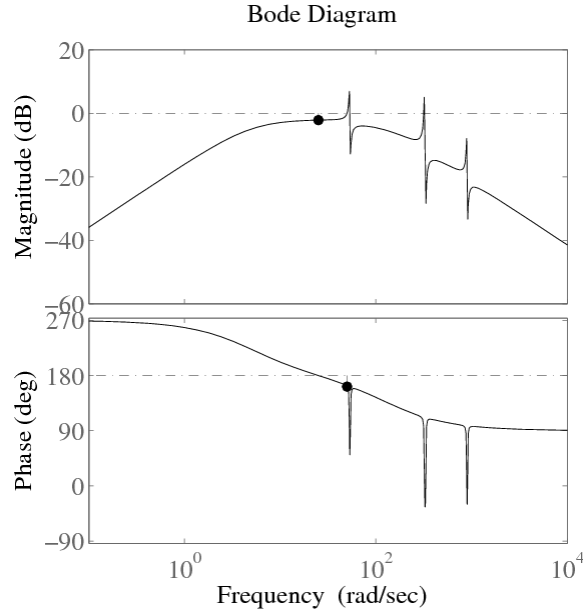
Figure 7. Bode diagram of $-C(s)G_{yu}(s)$ where $D_fK = 226.2$ and $1/D_f = -18$
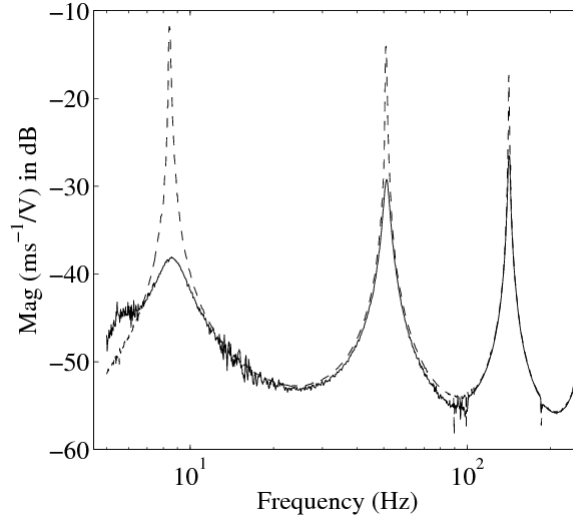
Figure 8. Measured open-loop (- -) and closed-loop (——) FRF of G_{zw} for the first three vibration modes

cy modes as well. In Table 1, the obtained attenuations for the first nine vibration modes are shown. Fig 9(b) shows the step response of G_{yw} for undamped and damped cases. We can observe that with our implemented analog IRC scheme, a damping of 26 dB is achieved at the first mode and the higher modes also show significant damping.

Table 1. Damping for the first nine modes of the cantilever beam

Mode number	1	2	3	4	5	6	7	8	9
Frequency [Hz]	8.4	51	141	276	463	687	972	1300	1663
Atenuation [dB]	26.2	15.2	9.2	4.5	7.4	0.9	2	2	2

4. CONCLUSION

A successful analog implementation of the IRC scheme was carried out and tested. This implementation was shown to be a simple single op-amp circuit that performed as per simulated predictions. A damping of up to 26 dB was achieved for the first mode. Higher frequency modes were also damped to various degrees. It is clear from these results that the IRC scheme has great potential in many industrial applications pertaining to vibration damping of collocated smart structures.
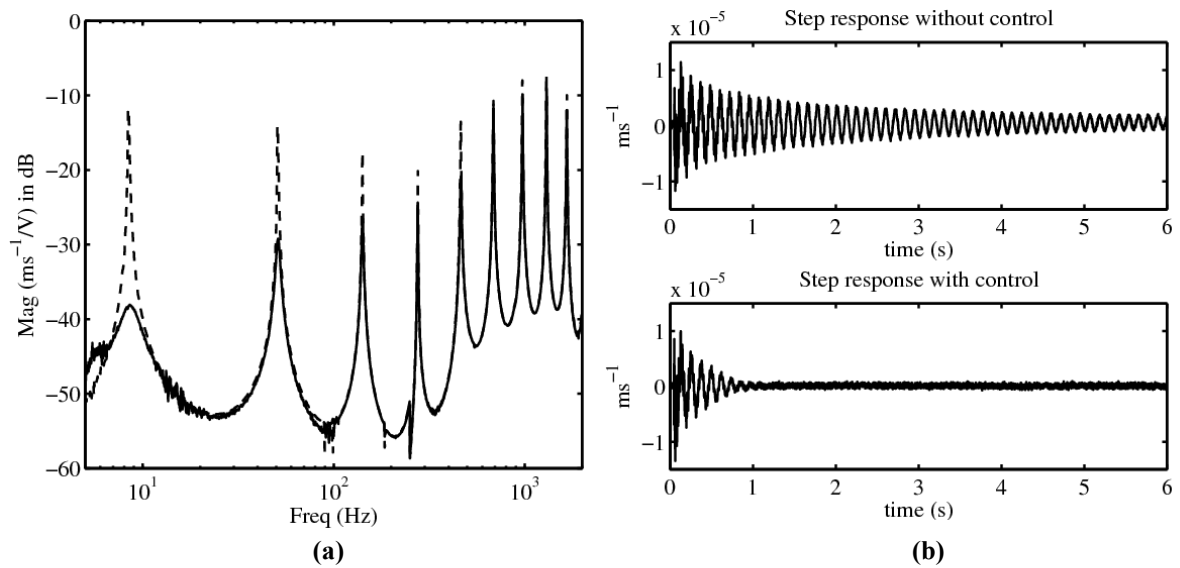
Figure 8. (a) Measured open-loop (- -) and closed-loop (—) FRF of G_{zw} for the first nine vibration mode. (b) Experimental open-loop (- -) and closed-loop(—) step responses of G_{zw} for a 20 V step input

ACKNOWLEDGEMENTS

REFERENCES

1. Tokhi, M., Mohamed Z. and Shaheed M., "Dynamic characterisation of a flexible manipulator system," *Robotica*, Vol. 18, pp. 571–80, (2001).
2. Han S. S., Choi S. B., and Kim H. H., "Position control of a flexible gantry robot arm using smart material actuators," *Journal of Robotics Systems*, Vol. 16, no. 10, pp. 581–595, (1999).
3. Cannon R. and Schwitz E., "Precise control of flexible manipulators," *Robotics Research: The First International Symposium*, ed. M Brady and R Paul (Cambridge, MA: MIT Press), (1984).
4. Wu S., Turner T. L. and Rizzi S. A., "Piezoelectric shunt vibration damping of an F-15 panel under high-acoustic excitation," *in Proc SPIE Smart Structures and Materials: Damping and Isolation*, pp. 276–287, (2000).
5. Benosman M. and Vey G., "Control of flexible manipulators: A survey," *Robotica*, Vol. 22, pp. 533–545, (2004).
6. Salapaka S., Sebastian A., Clevland J. P. and Salapaka M., "Design identification and control of a fast nanopositioning device," *in Proceedings of American Control Conference*, pp. 1966–1971 (2002).
7. Vaillon L. and Philippe C., "Passive and active microvibration control for very high pointing accuracy space systems," Smart Materials and Structures, Vol. 8, pp. 719–728, (1999).
8. Balas M. J., "Feedback control of flexible system," *IEEE Transactions on Automatic Control Engineering Practice*, Vol. 23, pp. 673–679, (1978).
9. Pota H. R. and Moheimani S. O. R., "Resonant controllers for smart structures," Smart Materials and Structures, Vol. 11, pp. 1–8, (2002).
10. Moheimani S. O. R. and Halim D., "Spatial resonant control of flexible structures - application to a piezoelectric laminated beam," *IEEE Transactions on Control Systems Technology*, Vol. 9(1), pp. 37–53, (2001).

11. Moheimani S. O. R. and Vautier B. J. G., "Resonant control of structural vibration using charge-driven piezoelectric actuators," *IEEE Transactions on Control System Technology*, Vol. 13(6), pp. 1021–1035, (2005).

12. Fanson J. L. and Caughey T. K., "Positive position feedback-control for large space structures," *AIAA Journal*, Vol. 28(4), pp. 717–724, (1990).

13. Moheimani S. O. R., Vautier B. J. G. and Bhikkaji B., "Experimental implementation of extended multi-variable PPF control on an active structure," *IEEE Transactions on Control Systems Technology*, Vol. 14(3), pp. 443–445, (2006).

14. Aphale S. S., Fleming A. J. and Moheimani S. O. R., "Integral resonant control of collocated smart structures," *Smart Materials and Structures*, Vol. 16, pp. 439–446, (2007).

15. Martin G. D., "On the control of flexible mechanical systems," Ph.D. dissertation, Stanford University, (1978).

16. Preumont A., Vibration control of active structures: an introduction. Dordrecht: The Netherlands, Kluwer Academic, (1997).

17. Hughes P. C., "Space structure vibration modes: how many exist? which ones are important?" *IEEE Control System Magazine*, Vol. 8, pp. 22–28, (1987).

18. Clark R. L., "Accounting for out-of-bandwidth modes in the assumed modes approach: implications on collocated output feedback control," *Transactions of the ASME, Journal of Dynamic Systems, Measurement, and Control*, Vol. 119, pp. 390–395, (1997).

19. Horowitz P. and Hill W., The art of electronics. Cambridge University Press, (1989).

20. Lanzon A. and Petersen I. R., "A modified positive-real type stability condition," *in Proceedings of the European Control Conference*, pp. 3912–3918 (July 2007).

21. McKelvey T., Akay L. and Ljung H., "Subspace based multivariable system identification from frequency response data," *IEEE Transactions on Automatic Control*, Vol. 41, pp. 960–978, (1996).